

Isolated Quasi-Switched-Capacitor DC/DC Converter using solar PV

Sathish kumar. T¹ PG Scholar, Dr. Balachandran. M² associate professor,

Department of EEE, nandha engineering college, erode, India

sathishkumar.ts.t7@gmail.com, balachandran_pm@yahoo.com

Abstract— This paper proposed to utilize the DC source from the solar PV. The DC/DC converter is the unidirectional power flow between the solar PV and load, while in existing its bidirectional. The proposed converter becomes compact using wide band gap devices which provide high efficiency and reduces heat generation of the circuit. PSO is used for the switching control for the converter. The converter can step up, step down and current doublers, synchronous rectifier is also present. The load can be a DC motor.

Keywords— unidirectional, solar PV, PSO, DC motor

INTRODUCTION

Now a day's use of other fossil fuels was becoming global warming and also due to lagging of the conventional fuels, the renewable sources plays major role throughout. Therefore the solar PV is used as a source for the converter unit. In the EV/HEV power system, a dc/dc converter is required to serve as an auxiliary power supply, connecting the high-voltage (HV) battery and the low voltage (LV) dc bus [2]. The LV dc bus is linked to the 12-V battery and the LV electronic loads such as the head lamps, stereo system, and various electronic control modules.

In normal operation, the converter delivers power from the HV battery to the LV electronic loads, while the 12-V battery is used only for stabilizing the voltage and starting up the vehicle. The converter must incorporate galvanic isolation to protect the LV electronic system from potentially hazardous high voltage [3]. For this application, full-bridge and half-bridge-based topologies, such as the phase-shift and resonant converters, are primarily considered as standard approaches [4]–[12]. In these topologies, the voltage stresses on the HV-side switches and the transformer HV-side winding equal to the HV-dc-bus voltage. Traditional fly back converter is not a suitable topology for this application mainly because of the dc-offset current in the transformer. In [13] and [14], new dc/dc converters derived from fly back topology were proposed, but the voltage stress on the HV-side switches is higher than the HV-dc-bus voltage. In HEVs/EVs, the HV-battery voltage is typically rated at about 350 V, and it can reach up to 450 V in fluctuations. In heavy-duty vehicles, the HV-battery voltage can be even higher. As the HV-battery voltage increases, the raised voltage stresses on components will lead to a lower efficiency of the converter and less component selection choices. Three-level dc/dc converters have been proposed in [15] and [16], having the ability to reduce the voltage stresses on HV-side switches by half. However, such converters require multiple components and complex control. Another approach to reduce the voltage stresses on switches is to apply the switched-capacitor circuit. In [17]–[20], new dc/dc converters based on switched-capacitor circuit are proposed. However, in the case of a higher HV-dc-bus voltage, these converters can only operate within a limited duty-ratio range, and will suffer severe current stresses in the components.

This paper proposes the unidirectional flow between the solar PV and the load. Aiming the good efficiency and to serve the converter for the certain applications. Now, the converter is proposes to run the DC motor applications. The features of the proposed converter include: 1) the voltage stresses on HV side switches are reduced to two-third of the HV-dc-bus voltage; 2) the voltage stress on transformer is reduced to one-third of the HV-dc-bus voltage; 3) the transformer turns ratio is reduced; 4) it has soft-switching capability and high efficiency; the block diagram for the above converter is shown in fig 1.

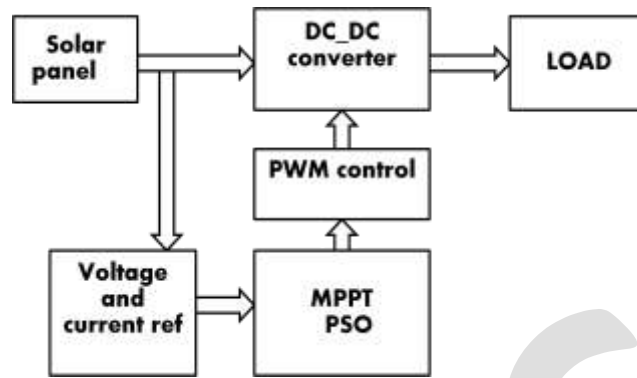


Figure 1: Block diagram

II. BLOCK MODEL-DESCRIPTION

A. solar PV

Photovoltaic cells are devices that absorb sunlight and convert that solar energy into electrical energy. Solar cells are commonly made of silicon, one of the most abundant elements on Earth. When photons (sunlight) hit a solar cell, its energy frees electron-holes pairs. The electric field will send the free electron to the N side and hole to the P side. This causes further disruption of electrical neutrality, and if an external current path is provided, electrons will flow through the path to their original side (the P side) to unite with holes that the electric field sent there, doing work for us along the way. The electron flow provides the current, and the cell's electric field causes a voltage.

Three solar cell types are currently available: mono-crystalline, polycrystalline, and thin film, discerned by material, efficiency, and composition.

B. MPPT

The Maximum Power Point Tracker (MPPT) is needed to optimize the amount of power obtained from the photovoltaic array to the power supply. MPPT is designed to withstand the harsh, fast changing environmental conditions of solar PV.

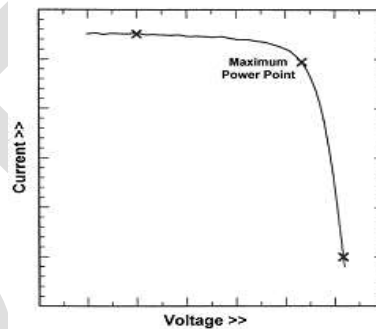


Figure 2: I-V Curve

Design of the customized MPPT will ensure that the system operates as closely to the Maximum Power Point (MPP) while being subjected to the varying lighting and temperature. The inputs of the MPPT consisted of the photovoltaic voltage and current outputs. The adjusted voltage and current output of the MPPT charges the power supply. A microcontroller was utilized to regulate the integrated circuits (ICs) and calculate the maximum power point, given the output from the solar array. Hardware and software integration was necessary for the completion of this component. While here the PSO is used as the advanced method for the substitute for microcontroller.

C. PSO

PSO adapts in searches for the best solution-vector in the search space. A single solution is called particle. Each particle has a fitness/cost value that is evaluated by the function to be minimized, and each particle has a velocity that directs the "flying" of the

particles. The particles fly through the search space by following the optimum particles. The algorithm is initialized with particles at random positions, and then it explores the search space to find better solutions. In every iteration, each particle adjusts its velocity to follow two best solutions. The first is the cognitive part, where the particle follows its own best solution found so far. This is the solution that produces the lowest cost (has the highest fitness). This value is called pBest (particle best). The other best value is the current best solution of the swarm, i.e., the best solution by any particle in the swarm. This value is called gBest (global best). Then, each particle adjusts its velocity and position with the following equations:

$$v' = v + c1.r1. (pBest - x) + c2.r2. (gBest - x)$$

$$x' = x + v'$$

v is the current velocity, v' the new velocity, x the current position, x' the new position, pBest and gBest as stated above, $r1$ and $r2$ are even distributed random numbers in the interval $[0, 1]$, and $c1$ and $c2$ are acceleration coefficients. Where $c1$ is the factor that influences the cognitive behavior, i.e., how much the particle will follow its own best solution and $c2$ is the factor for social behavior, i.e., how much the particle will follow the swarm's best solution.

D. WBG

Wide band gap devices are operates at higher frequencies to filter the harmonics. This also employs to minimize the size of the passive component particularly for the switched capacitor. It has been documented extensively in the literature that WBG devices have lower switching loss, better reverse recovery characteristics, and lower figure of merit in terms of the product of $R_{ds(on)}$ and total gate charge Q_g [22]–[23].

Wide band gap devices provide good efficiency.

In the existing system the wide band gap devices are designed to withstand the harsh condition due to the temperature developed in the vehicles [1]. Such kind of protection is not necessary for the proposed converter.

III. OPERATION PRINCIPLE OF PROPOSED ISOLATED QSC CONVERTER

A. Circuit Description:

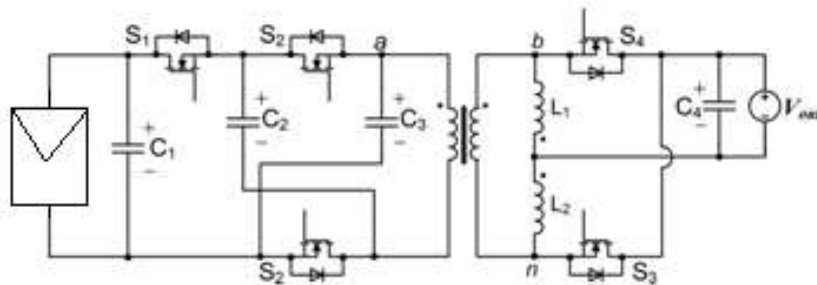


Figure 3: proposed isolated quasi switched capacitor

The power supply is utilized from the solar PV. The $L1$ and $L2$ are the shunt connect with Lm . Inductances of Lm is much greater than $L1$ and $L2$. Thus the transformer can

withstand without any air-gap. The proposed converter can operates in various modes according to the duty cycle given to the circuit. Based on that duty cycle ratio the converter modes are as follows.

$\delta < 50\%$ - Buck mode

$\delta > 50\%$ - Boost mode

B. Buck mode operation:

The buck mode operation can be explained based on the various switching frequencies.

(i) **Hard switching operation:**

Switches S1- S4 and S2-S3 are the two complementing pairs.

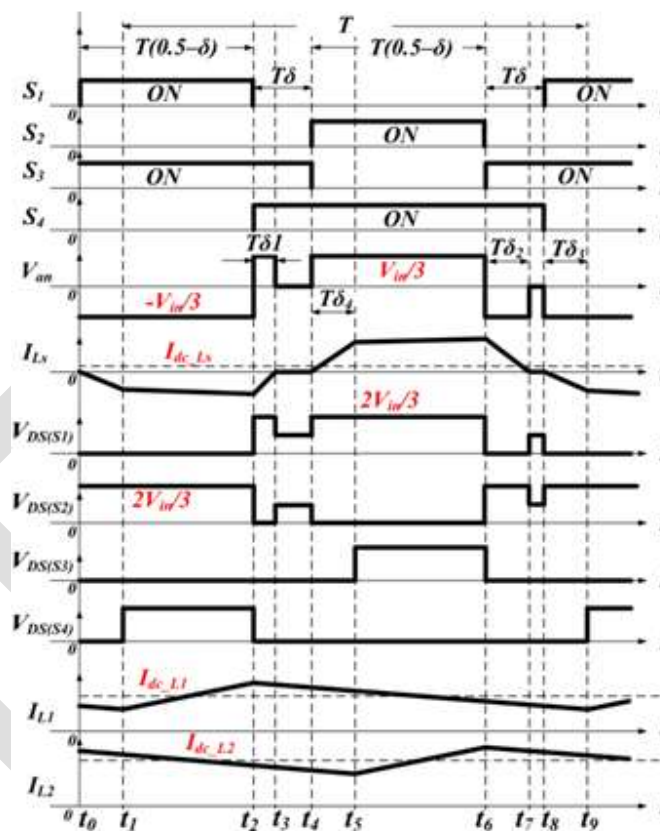


Figure 4: hard switching operation of buck mode.

Mode 1 ($t_1 - t_2$): The input voltage source, C2, C3, Ls, L1, and L2 are connected in series. C2 and C3 are charged. L1 and Ls store energy, while L2 release its energy to the load.

Mode 2 ($t_2 - t_3$): Ls releases its energy back to C2 and C3, via S3, S4, and the body diode of S2. L1 and L2 release their energy to the load.

Mode 3 ($t_3 - t_4$): The energy of Ls is completely released at t_3 . The body diode of S2 is blocked. L1 and L2 continue to release their energy to the load.

Mode 4 ($t_4 - t_5$): C_2 and C_3 are connected in parallel and they are discharged. L_1 and L_2 continue to release their energy to the load. Both V_{L1} and V_{L2} are clamped to the output voltage, so I_{Ls} increases quickly, transferring the current flowing through S_3 to S_4 . The body diode of S_3 conducts because the current of I_{L2} is larger than I_{Ls} .

Mode 5 ($t_5 - t_6$): The current of I_{L2} is equal to I_{Ls} at t_5 , so the current of S_3 reaches 0 at t_5 . After t_5 , the body diode of S_3 is blocked.

Mode 6 ($t_6 - t_7$): L_s releases its energy back to the input voltage source and C_1 , via S_3 , S_4 , and the body diodes of S_1 ; L_1 and L_2 release their energy to the load.

Mode 7 ($t_7 - t_8$): The energy of L_s is completely released. The body diode of S_1 is blocked. L_1 and L_2 continue to release their Energy.

Mode 8 ($t_8 - t_9$): The input voltage source, C_2 , C_3 , L_s , L_1 , and L_2 are connected in series. Both V_{L1} and V_{L2} are clamped to the output voltage, so I_{Ls} increases quickly, transferring the current flowing through S_4 to S_3 . During this mode, the body diode of S_4 conducts because the current of I_{L1} is larger than I_{Ls} . At t_9 , the current of S_4 reaches 0 and its body diode is blocked.

(ii) Soft switching operation:

The converter has the capability to realize ZVS in the front stage circuit and ZCS in the post-stage circuit. To achieve the ZVS ON of S_1 and S_2 , the freewheeling current must continue to flow till the dead-band transients are over, which means the switching Mode 3 and Mode 7 must be bypassed. Fig. 5 shows the major waveforms of the buck-mode, soft-switching operation.

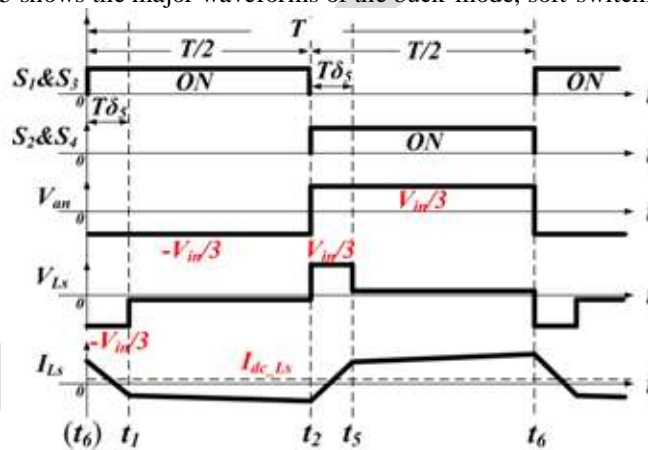


Figure 5: soft switching operation of buck mode.

In Fig. 5, $T\delta_5$ is the freewheeling transient, where L_s releases and stores energy. During $T\delta_5$, S_1 or S_2 is turned ON for enabling synchronous rectification that reduces the conduction loss. Based on the volt-second balance of L_1 , the δ_5 is derived as,

$$\delta_5 = \frac{(V_{in} - 3N \cdot V_{out}) \cdot N^2 L_1 - 3N \cdot V_{out} \cdot (N^2 L_1 + L_s)}{2[3N \cdot V_{out} \cdot (N^2 L_1 + L_s) + (V_{in} - 3N \cdot V_{out}) \cdot N^2 L_1]}$$

C. Boost mode operation:

Soft switching operation:

In boost mode, the duty ratios of S_1 and S_2 are fixed at 50%. The duty ratios of S_3 and S_4 need be extended over 50%, to overlap in advance with those of S_1 and S_2 , respectively. In the overlapped transients, the transformer leakage inductance stores and releases energy which is required for boost-mode power delivery. Fig. 6 shows the major waveforms of the boost mode, soft-switching operation. Similarly, based on the voltage and the current of L_s at different time, P_o of the boost mode operation can be derived as,

$$P_o = \left[\frac{(V_{out}^2 - 3NV_{in}V_{out})}{9(N^2 L_1 + L_s)} - \frac{V_{out}^2}{9L_s} \right] \cdot \left(\frac{1}{2} - \delta_6 \right) \cdot \delta_6 \cdot \frac{1}{f_s}$$

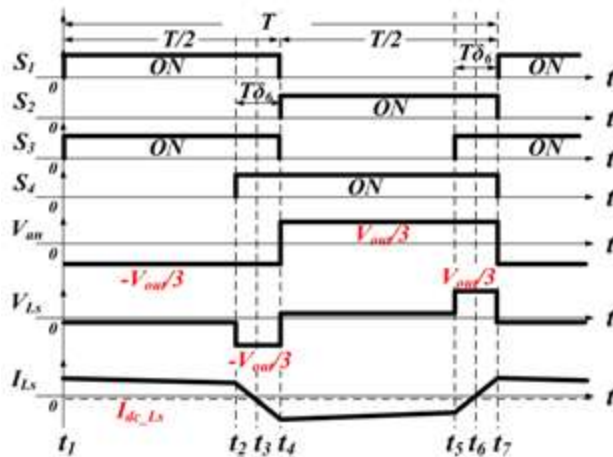


Figure 6: soft switching operation of boost mode.

IV. SIMULATION RESULTS

The simulation is done by using the MATLAB software, in which the converter has the solar PV, was completely controlled by the MPPT technique to maintain the constant power to the converter. PSO serves in the MPPT technique to get the accurate result of the converter.

Experimental results:

1. The converter efficiency increased.
2. The voltage stress of is reduced.
3. Solar intensities were different but the result will be the constant DC voltage is possible.
4. Converter made into compact size.

CONCLUSION

This paper proposes the isolated quasi switched capacitor DC/DC converter for the effective utilization of the unidirectional power flow between the solar PV and DC motor. By the use of converter the voltage stress has been reduced to the level and the wide band gap devices employs to better performance of the converter and to avoid the generation of heat to the converter. Thus the efficiency of the converter is higher than the existing model and it values 96.4%. which means it provides the higher switching frequencies.

REFERENCES

- [1] Xuan Zhang., Chengcheng Yao, Cong Li, Lixing Fu, Feng Guo, " A Wide Bandgap Device-Based Isolated Quasi-Switched-Capacitor DC/DC Converter ", *IEEE transactions on power electronics*, vol. 29, no. 5, MAY 2014.
- [2] A. Emadi, S. S. Williamson, and A. Khaligh, "Power electronics intensive solutions for advanced electric, hybrid electric, and fuel cell vehicular power systems," *IEEE Trans. Power Electron.*, vol. 21, no. 3, pp. 567– 577, May 2006.
- [3] A. Gogerino, A. Guerra, D. Kinzer, and J. Marcinkowski, "Comparison of High Voltage Switches in Automotive DC-DC Converter," in *Proc. Power Convers. Conf. - Nagoya, Apr. 2007*, pp. 360–367.
- [4] F. Z. Peng, H. Li, G. Su, and J. S. Lawler, "A new ZVS bidirectional DCDC converter for fuel cell and battery application," *IEEE Trans. Power Electron.*, vol. 19, no. 1, pp. 54–65, Jan. 2004.
- [5] F. Krömer and J. W. Kolar, "Efficiency-optimized high-current dual active bridge converter for automotive applications," *IEEE Trans. Ind. Electron.*, vol. 59, no. 7, pp. 2745–2760, Jul. 2012.
- [6] J. Lee, Y. Jeong, and B. Han, "A two-stage isolated/bidirectional DC/DC converter with current ripple reduction technique," *IEEE Trans. Ind. Electron.*, vol. 59, no. 1, pp. 644–646, Jan. 2012.
- [7] T. Wu, Y. Chen, J. Yang, and C. Kuo, "Isolated bidirectional full-bridge DC–DC converter with a flyback snubber," *IEEE Trans. Power Electron.*, vol. 25, no. 7, pp. 1915–1922, Jul. 2010.
- [8] M. Pahlevaninezhad, P. Das, J. Drobnik, P. K. Jain, and A. Bakhshai, "A novel ZVZCS full-bridge DC/DC converter used for electric vehicles," *IEEE Trans. Power Electron.*, vol. 27, no. 6, pp. 2752–2769, Jun. 2012.
- [9] L. Zhu, "A novel soft-commutating isolated boost full-bridge ZVS-PWM DC-DC converter for bidirectional high power applications," in *Proc. IEEE 35th Annu. Power Electron. Spec. Conf.*, Jun. 2004, vol. 3, pp. 2141– 2146.
- [10] S. Han and D. Divan, "Bi-Directional DC/DC converters for Plug-in hybrid electric vehicle (PHEV) applications," in *Proc. Twenty-Third Annu. IEEE Appl. Power Electron. Conf. Expo.*, Feb. 2008, pp. 784–789.

- [11] G. Pledl, M. Tauer, and D. Buecherl, "Theory of operation, design procedure and simulation of a bidirectional LLC resonant converter for vehicular applications," in *Proc. IEEE Vehicle Power Propulsion Conf.*, Sep. 2010, pp. 1–5.
- [12] B. Lin and C. Chao, "Soft switching converter with two series half-bridge legs to reduce voltage stress of active switches," *IEEE Trans. Ind. Electron.*, vol. 60, no. 6, pp. 2214–2224, Jun. 2013.
- [13] E. V. de Souza and I. Barbi, "Bidirectional current-fed flyback-push-pull DC-DC converter," in *Proc. Brazilian Power Electron. Conf.*, Sep. 2011, pp. 8–13.
- [14] T. Bhattacharya, V. S. Giri, K. Mathew, and L. Umanand, "Multiphase bidirectional flyback converter topology for hybrid electric vehicles," *IEEE Trans. Ind. Electron.*, vol. 56, no. 1, pp. 78–84, Jan. 2009.
- [15] P. Li, W. Li, Y. Zhao, H. Yang, and X. He, "ZVS three-level phase-shift high step-down DC/DC converter with two transformers," in *Proc. 14th Eur. Conf. Power Electron. Appl.*, Aug. 2011, pp. 1–10.
- [16] B.-R. Lin and C.-H. Chao, "Analysis of an interleaved three-level ZVS converter with series-connected transformers," *IEEE Trans. Power Electron.*, vol. 28, no. 7, pp. 3088–3099, Jul. 2013.
- [17] A. A. Fardoun, E. H. Ismail, A. J. Sabzali, and M. A. Al-Saffar, "Bidirectional Converter with Low Input Output Current Ripple for Renewable Energy Applications," in *Proc. Third Annu. IEEE Energy Convers. Congr. Expo.*, Sept. 2011, pp. 3322–3329.
- [18] A. A. Fardoun and E. H. Ismail, "SEPIC converter with continuous output current and intrinsic voltage doubler characteristic," in *Proc. IEEE Int. Conf. Sustainable Energy Technol.*, Nov. 2008, pp. 431–436.
- [19] H. Nomura, K. Fujiwara, and M. Yoshida, "A New DC-DC converter circuit with larger step-up/down ratio," in *Proc. 37th IEEE Power Electron. Spec. Conf.*, Jun. 2006, pp. 1–7.
- [20] B. Axelrod, Y. Berkovich, and A. Ioinovici, "Switched capacitor/switched-inductor structures for getting transformer less hybrid DC-DC PWM converters," *IEEE Trans. Circuits Syst. I: Reg. Papers*, vol. 55, no. 2, pp. 687–696, Mar. 2008.
- [21] Y.-K. Lo, J.-Y. Lin, and C.-Y. Lin, "Asymmetrical zero-voltage-switching PWM DC-DC converter employing two transformers and current doublers rectification," *IET Power Electron.*, vol. 1, no. 3, pp. 408–418, Sep. 2008.
- [22] B. Callanan, 2011. "Application considerations for silicon carbide MOSFETs," [Online]. Available: <http://www.cree.com/~media/Files/Cree/Power/Application%20Notes/CPWRAN08.pdf>
- [23] D. Reusch and J. Strydom, "Understanding the effect of PCB layout on circuit performance in a high frequency gallium nitride based point of load converter," *IEEE Trans. Power Electron.*, vol. 29, no. 4, pp. 2008–2015, Apr. 2014.